JPET Fast Forward. Published on May 9, 2014 as DOI: 10.1124/jpet.114.214189
This article has not been copyedited and formatted. The final version may differ from this version.

JPET #214189

Title Page

Trovafloxacin enhances LPS-stimulated production of TNF by macrophages: role of the DNA damage response

Kyle L. Poulsen, Jesus Olivero Verbel, Kevin M. Beggs, Patricia E. Ganey and Robert A. Roth

Department of Pharmacology & Toxicology, Center for Integrative Toxicology, Michigan State University, East Lansing, MI 48824-1302 (*KLP, KMB, PEG and RAR)*; Environmental and Computational Chemistry Group, School of Pharmaceutical Sciences, University of Cartagena, Cartagena, Colombia (*JO*)

Running Title Page

Running Title: Trovafloxacin-induced TNF production

Corresponding author: Robert A. Roth, Department of Pharmacology & Toxicology, Center for Integrative Toxicology, Michigan State University, Food Safety and Toxicology Building, 1129 Farm Lane, Room 221, East Lansing, MI 48824. Tel: (517) 353-9841. Fax: (517) 432-2310. rothr@msu.edu

Text pages: 18

Figures: 7 total (1 supplemental)

Abstract word count: 247

Introduction word count: 653

Discussion word count: 1276

References cited: 44

Abbreviations used:

ATM - ataxia telangiectasia mutated

ATR - ATM and Rad3-related

CPX - ciprofloxacin

DDR - DNA damage response

DSB - double-strand DNA breaks

IDILI - Idiosyncratic, drug-induced liver injury

kDNA - kinetoplastid DNA

LPS - lipopolysaccharide

LVX - levofloxacin

MOX - moxifloxacin

pATM/ATR substrate - phosphorylated-(Ser/Thr) ATM/ATR substrate

pH2A.X - phosphorylated histone 2A.X

PI3K - phosphoinositide 3-kinase

RAW cells - RAW 264.7 murine macrophages

TNF - tumor necrosis factor-alpha

TopIIa - eukaryotic topoisomerase II-alpha

TVX - trovafloxacin

WORT - wortmannin

Abstract

Trovafloxacin (TVX) is a drug that has caused idiosyncratic, drug-induced liver injury (IDILI) in humans. In a murine model of IDILI, otherwise nontoxic doses of TVX and the inflammagen, lipopolysaccharide (LPS), interacted to produce pronounced hepatocellular injury. The liver injury depended on a TVX-induced, small but significant prolongation of tumor necrosis factor-alpha (TNF) appearance in the plasma (Shaw et al., 2009ab). The enhancement of TNF expression by TVX was reproduced in vitro in RAW 264.7 murine macrophages (RAW cells) stimulated with LPS. The current study was designed to identify the molecular target of TVX responsible for this response in RAW cells. An *in silico* analysis suggested a favorable binding profile of TVX to eukaryotic topoisomerase II-alpha (TopIIa), and a cell-free assay revealed that TVX inhibited eukaryotic TopIIa activity. Topoisomerase inhibition is known to lead to DNA damage, and TVX increased the DNA damage marker phosphorylated H2A.X in RAW cells. Moreover, TVX induced activation of the DNA damage sensor kinases, ataxia telangiectasia mutated (ATM) and Rad3-related (ATR). The ATR inhibitor NU6027 prevented the TVX-mediated increases in LPS-induced TNF mRNA and protein release, whereas a selective ATM inhibitor (KU55933) was without effect. TVX prolonged TNF mRNA stability, and this effect was largely attenuated by NU6027. These results suggest that TVX can inhibit eukaryotic topoisomerase, leading to activation of ATR and potentiation of TNF release by macrophages, at least in part through increased mRNA stability. This off-target effect might contribute to the ability of TVX to precipitate IDILI in humans.

JPET Fast Forward. Published on May 9, 2014 as DOI: 10.1124/jpet.114.214189
This article has not been copyedited and formatted. The final version may differ from this version.

Introduction

Idiosyncratic, drug-induced liver injury (IDILI) is an adverse response to numerous pharmaceuticals. IDILI is responsible for approximately 13% of all cases of acute liver failure (Ostapowicz et al., 2002) and for many of the FDA-imposed restrictions on drug use (Lasser et al., 2002). Although typically rare, these reactions cause significant morbidity and mortality and pose a financial burden to pharmaceutical companies when offending drugs must be withdrawn from the market (Shaw et al., 2007). Although drugs from several pharmaceutical classes have been associated with human IDILI, many are antibiotics. For example, in the class of broad-spectrum, fluoroquinolone antibiotics, trovafloxacin (TVX), ciprofloxacin (CPX) and moxifloxacin (MOX) have caused IDILI in human patients, whereas levofloxacin (LVX) has shown little to no such liability (Leitner et al., 2010).

Several hypotheses have emerged to explain IDILI, yet none has been proven conclusively (Shaw et al., 2010). One hypothesis states that a transient inflammatory episode can interact with a normally nontoxic dose of a drug to bring about liver injury. Rodent models of IDILI based on this inflammatory stress hypothesis have been developed for several drugs, including TVX, sulindac, amiodarone and others (Roth and Ganey, 2011). In these models, drugs associated with IDILI in humans synergize with an inflammagen such as lipopolysaccharide (LPS) to precipitate hepatotoxicity. At the doses used in these models, LPS exposure prompts an early increase in tumor necrosis factor-alpha (TNF) in the plasma but no liver necrosis. IDILI-associated drugs do not by themselves cause liver injury or TNF expression, but coadministration of drug with LPS causes a small prolongation of the LPS-stimulated TNF appearance that is critical to the

pathogenesis of liver injury in cotreated animals (Lu et al., 2012; Shaw et al., 2007; Shaw et al., 2009a; Zou et al., 2009).

An example is a murine model involving TVX/LPS coexposure. TVX is not hepatotoxic in mice even when given at large doses. However, when mice were cotreated with TVX and an otherwise nontoxic dose of LPS, pronounced hepatocellular necrosis occurred. Interestingly, this hepatotoxic interaction with LPS did not occur upon cotreatment with LVX. The liver injury from LPS/TVX cotreatment was absent in TNF receptor knockout mice or when TNF was neutralized by etanercept treatment (Shaw et al., 2007; Shaw et al., 2009b). Importantly, when etanercept was administered at the peak of LPS-stimulated TNF appearance to prevent the prolongation of TNF appearance in TNF/LPS-cotreated mice, liver injury was prevented. Thus, although the prolongation was relatively brief and the increase was minor in magnitude compared to that which occurred from LPS alone, it was required for hepatotoxicity (Shaw et al., 2007; Shaw et al., 2009b).

Examination of the TVX-LPS interaction in the murine model in vivo did not reveal a specific molecular target of TVX. The enhancement of LPS-stimulated TNF release by TVX could arise from a direct effect of the drug on TNF-producing cells in the liver. Indeed, pretreatment of murine RAW 264.7 cells (RAW cells) with TVX potentiated LPS-induced TNF release (Poulsen et al., 2014). Thus, the influence of TVX on LPS-stimulated TNF appearance that occurs in vivo was recapitulated in a macrophage cell line, thereby providing an in vitro system that can be employed to evaluate mechanisms of the LPS-drug interaction.

The antibiotic activity of the fluoroquinolones derives from their ability to inhibit bacterial topoisomerases and gyrases (Brighty and Gootz, 1997). Interestingly, in addition to their ability to inhibit prokaryotic topoisomerases, fluoroquinolones TVX, CPX and MOX have weak inhibitory activity against eukaryotic topoisomerase II-alpha (TopIIa) (Albertini et al, 1995; Barrett et al., 1989; Herbold et al., 2001; Reuveni et al., 2008). It is well recognized that inhibiting ("poisoning") topoisomerases can lead to DNA damage (Drummond et al., 2011; Ryan et al., 1991). DNA damage prompts intracellular signaling involving activation of kinases that might enhance TNF expression. Accordingly, we tested the hypothesis that potentiation of LPS-induced TNF production in RAW cells by TVX results from topoisomerase inhibition and the consequent DNA damage response.

JPET Fast Forward. Published on May 9, 2014 as DOI: 10.1124/jpet.114.214189
This article has not been copyedited and formatted. The final version may differ from this version.

Methods

Chemicals and Inhibitors

All chemicals and reagents were purchased from Sigma-Aldrich (St. Louis, MO) unless stated otherwise. Antibiotic/antimycotic and DMEM were purchased from Life Technologies (Grand Island, NY). KU55933 was purchased from Tocris Bioscience (Bristol, United Kingdom).

In silico docking of TVX and LVX to topoisomerase II-alpha (TopIIa)

The docking routine of TVX and LVX onto TopIIa consisted of 1) ligand optimization, 2) protein preparation and 3) protein-ligand docking. A brief description of each procedure follows: 1) The 3D geometries of TVX and LVX were optimized using Density Functional Theory (DFT), employing the B3LYP/6-31G basis set, and calculations were carried out with the Gaussian 03 software package (Vreven et al., 2003). Open Babel was used to transform optimized geometries to Mol2 format for subsequent processing (Guha et al., 2006). 2) Experimental coordinates of the X-ray crystallographic structure of TopIIa (PDB ID: 1ZXN, chains A and B) were downloaded from Protein Data Bank (PDB). Sybyl-X 2.0 Suite (SYBYL-X 2.0, Molecular modeling software 2012, Tripos. St. Louis, MO) was employed to prepare protein structures for molecular docking. During this process ligands and water molecules were removed, side chains repaired, and hydrogen atoms added to the protein. The binding sites for the ligands on TopIIa were defined utilizing MGL Tools 1.5.0 (Sanner et al., 1999) by forming a cube with the dimensions 86 × 70 × 90 Å, engulfing the whole protein

JPET Fast Forward. Published on May 9, 2014 as DOI: 10.1124/jpet.114.214189
This article has not been copyedited and formatted. The final version may differ from this version.

structure, using a grid point spacing of 1.0 Å and center grid boxes of 63.249, 3.440 and 58.618, in X, Y and Z coordinates, respectively. 3) Molecular docking methods were employed to model the ability of TVX and LVX structures to form complexes with TopIIa. Protein-ligand docking calculations were performed with AutoDock Vina 1.0 program (Trott and Olson, 2010). All calculations with AutoDock Vina included 20 number modes, an energy range of 1.5, and exhaustiveness equal to 25. Five hundred docking runs were executed for each ligand, saving the best-obtained pose for each one. The average binding affinity for these poses was computed as the affinity value for a given predicted complex. As the docking procedure allowed the identification of several binding sites within the same protein, *in silico* affinities, measured as Kcal/mol, were presented for each theoretical binding site suggested by AutoDock Vina.

Topoisomerase Decatenation Assay

TopIIa isoform activity was analyzed in the presence of VEH or TVX at various concentrations using etoposide as a positive control with the Human Toposiomerase II Assay Kit (TopoGEN Inc, Port Orange, FL). Briefly, 1 unit of human TopIIa was incubated with 200 ng kinetoplastid DNA (kDNA) in the presence of VEH or TVX in complete assay buffer at 37°C for 30 minutes. One unit of topoisomerase is defined as the amount of enzyme required to separate the highly catenated kDNA substrate at 37°C for 30 minutes. The reaction was stopped using the stop buffer provided, and the reaction products were loaded onto a 1% agarose gel for analysis of topoisomerase activity.

JPET Fast Forward. Published on May 9, 2014 as DOI: 10.1124/jpet.114.214189
This article has not been copyedited and formatted. The final version may differ from this version.

Cell Culture

RAW 264.7 macrophage-like cells (American Type Culture Collection, Manassas, VA) were maintained in DMEM supplemented with 10% heat-inactivated FBS and 1% antibiotic/antimycotic (Life Technologies) at 37°C in 5% CO_2. Cells were harvested by detachment with a sterile spatula and plated at a density of 4 X 10^4 cells per well in 24-well plates (Costar, Lowell, MA) for cytokine release and RNA isolation or 1.5 X 10^5 cells per well in 6-well plates (Costar). 24 h after plating, cells were synchronized by replacing medium with 0.5% FBS-containing medium. After overnight incubation, cells were exposed to drug. Exposure to TVX (100 µM) was not cytotoxic to RAW cells (3.6 +/- 0.6% release of LDH over 6 hours) in the absence or presence of LPS.

Quantitative Polymerase Chain Reaction (qPCR)

Total RNA was isolated from RAW cells using TRIzol reagent (Life Technologies). cDNA was prepared with the iScript cDNA synthesis kit using 1 µg of isolated RNA (Bio-Rad Laboratories, Hercules, CA). The expression level of TNF was analyzed using the StepOne Real-Time PCR machine and SYBR Green reagents for amplicon detection (Applied Biosystems, Foster City, CA). Expression level was normalized to beta actin (β-actin). TNF mRNA stability was assessed by treating cells with TVX or an equal volume of 0.1N KOH vehicle (VEH) for 1 hour before adding 5 µg/ml actinomycin D (ActD) to stop transcription. RNA was isolated at 15 minute-intervals after the addition of ActD and converted to cDNA, and TNF mRNA was measured and normalized to β-actin.

PCR primers used were: mouse TNF [5' -TCTCATGCACCACCATCAAGGACT-3' (forward) and 5' - ACCACTCTCCCTTTGCAGAACTCA- 3' (reverse)] and mouse β-actin [5' –TGTGATGGTGGGAATGGGTCAGAA- 3' (forward) and 5' – TGTGGTGCCAGATCTTCTCCATGT- 3' (reverse)].

Western Analysis

Cells were lysed in radioimmunoprecipitation assay (RIPA) buffer supplemented with HALT protease and phosphatase inhibitor cocktail (Thermo Scientific). Protein concentration in cell isolates was determined by the bicinchonic assay (BCA). Western analyses were performed by loading 20 µg of protein on precast NuPAGE® SDS-PAGE gels (Life Technologies) using all NuPAGE® reagents. Samples were separated on precast 12% gels. Separated proteins were transferred to polyvinylidene difluoride (PVDF) membranes (Millipore, Billerica, MA) for 1 hour at 4° C. Membranes were blocked in 5% BSA dissolved in tris-buffered saline plus 0.1% Tween20 (TBST) and then probed for phospho-(Ser/Thr) ATM/ATR substrate (pATM/ATR substrate)**,** phospho-histone H2A.X (Ser139) (Cell Signaling Technology, Boston, MA). Membranes were then stripped with Restore western blot stripping agent (Thermo Scientific) and reprobed for Lamin B1 (Abcam, Cambridge, MA).

Measurement of TNF Concentration

For determination of TNF protein in culture medium, an enzyme-linked immunosorbent assay (ELISA) was performed (BD Biosciences, San Jose, CA). Cell culture medium was withdrawn at various times and stored at -20°C until the time of

analysis. Ninety-six-well plates were coated with an anti-TNF capture antibody in a coating buffer overnight at 4°C. Medium was diluted to remain within standard curve concentrations.

Studies with inhibitors

Inhibitors KU55933 (Hickson et al., 2004), NU6027 (Peasland et al., 2011) and wortmannin (Powis et al., 1994) were dissolved in DMSO at a stock concentration of 10 mM and diluted to final concentrations in 0.5% FBS-containing medium. Inhibitors or an equivalent volume of DMSO vehicle were added at the moment RAW cells were exposed to VEH or TVX, unless noted otherwise.

Statistical Analysis

A one- or two-way Analysis of Variance (ANOVA) was performed on data sets with Tukey's post-hoc test applied for comparisons among groups. The criterion for significance was $p < 0.05$.

Results

TVX interaction with TopIIa: *in silico* analysis

Human TopIIa was selected for analysis because it is the eukaryotic homolog to prokaryotic DNA gyrase and topoisomerase IV (Bates et al., 2011; Drummond et al., 2011). TVX binding to eukaryotic TopIIa occurred at two binding sites (Figure 1A), the most frequently occupied of which (99.4%) was the one with the greatest predicted affinity (-9.3±0.0 Kcal/mol) (Figure 1B). In contrast, LVX was predicted to bind to TopIIa at three sites (Figure 1C). The site most frequently occupied by LVX (95%) (Figure 1D) differed from that to which TVX was most commonly bound. In addition, the absolute affinity for LVX binding to TopIIa (-8.5±0.0 Kcal/mol) was smaller than that observed for TVX. These results indicate that TVX is predicted to bind to eukaryotic TopIIa and does so at a different site and with greater affinity than LVX.

TVX inhibits TopIIa-dependent decatenation of kDNA

The ability of TVX to inhibit TopIIa-dependent decatenation of kDNA was evaluated in a cell-free assay (Figure 2). In this assay, decatenation of kDNA by TopIIa results in two distinct DNA catenates of different molecular weights that migrate through the agarose gel, whereas kDNA remains in the loading wells. In the absence of TopIIa (lane labeled kDNA), the kDNA does not migrate. As a positive control, VP-16, a potent inhibitor of human TopIIa, completely prevented kDNA decatenation. Although 10 μM TVX did not affect TopIIa, the presence of TVX at concentrations of 30 – 300 μM

decreased decatenated DNA products and increased kDNA retention as compared to VEH control containing only TopIIa. This indicated that TVX could inhibit eukaryotic topoisomerase at concentrations near those attained in the plasma during TVX therapy (Teng et al., 1996).

TVX increases DNA lesions in RAW 264.7 cells

Poisoning of topoisomerase activity in cells leads to several outcomes, one of which is the formation of double-stranded lesions in DNA (Drummond et al., 2011; Ryan et al., 1991). Phosphorylated histone 2A.X (pH2A.X) is a sensitive marker of DNA lesions and is induced rapidly after the onset of a lesion by the damage-sensing kinases, ataxia telangiectasia mutated (ATM) and ataxia telangiectasia mutated and Rad3-related (ATR) (Kastan et al., 2000). After a 2-hour incubation of RAW cells with TVX, pH2A.X increased in a concentration-dependent manner (Figure 3A). LVX, however, did not increase pH2A.X in RAW cells over the same duration of exposure (Figure 3B).

TVX activates ATM/ATR-dependent signaling

ATM and ATR are phosphoinositide 3-kinases (PI3Ks) that share a common minimal phosphorylation motif on protein substrates; i.e., a serine or threonine residue is phosphorylated if the amino acid occurs between leucine and glutamine (Kim et al., 1999). Incubation of RAW cells with TVX for 1 hour increased phosphorylation of a

substrate containing the minimal ATM/ATR phosphorylation motif (Figure 4A). This increase was absent after a 2-hour exposure to TVX. KU55933, a selective ATM inhibitor, and NU6027, an ATR-signaling inhibitor (Peasland et al., 2011), each prevented generation of the pATM/ATR substrate in VEH- or TVX-exposed RAW cells (Figure 4B), indicating that ATM- and ATR-dependent signaling was activated by TVX.

TVX increases TNF mRNA in an ATR-selective manner

As noted above, TNF is a critical factor in the pathogenesis of liver injury in TVX/LPS cotreated mice, and TVX increases TNF expression in LPS-stimulated RAW cells in vitro (Poulsen et al., 2014; Shaw et al., 2007). The influence of ATM and ATR activation on TVX-dependent TNF expression in RAW cells was assessed. TVX increased TNF mRNA after a two-hour exposure to the drug (Figure 5A). The increase in TNF mRNA was reduced by NU6027 but not by KU55933 or by the nonselective PI3K inhibitor, wortmannin (WORT).

One way that increases in mRNA can occur is by stabilization of the transcript. To address this possibility, RAW cells were exposed to TVX for one hour before adding ActD to prevent RNA synthesis. This time of ActD addition was chosen because it coincides with the TVX-mediated increase in ATR signaling (Figure 4A) but precedes the increase in TNF mRNA (seen at 2h; Figure 5A). TVX markedly increased the stability of TNF mRNA (Figure 5B), and NU6027 prevented this increased stability. This result suggested that the TVX-mediated increase in TNF mRNA depicted in Figure 5A was likely due to an ATR-dependent stabilization of TNF transcripts.

TVX increases LPS-induced TNF protein release in an ATR-dependent manner

The role of ATR in the TVX-mediated increase in TNF release from RAW cells was assessed next. As expected, LPS stimulated the release of TNF from RAW cells (Figure 6). TVX-pretreatment increased TNF release 3h after saline (SAL) or LPS exposure (Figure 6A, black bars). As found with TNF mRNA (Figure 5), the increase in TNF protein release was insensitive to KU55933 or WORT but was reduced by NU6027. In cells cotreated with TVX and LPS, NU6027 reduced TNF release to the level stimulated by LPS alone. Unlike the results after 3h, TNF release 6h after LPS exposure was largely unaffected by NU6027 (Figure 6B). At this time, NU6027 reduced the increase in TNF due to exposure to TVX alone but did not prevent the increase in LPS-induced TNF release caused by TVX pretreatment. Taken together, the results suggested that the TVX-mediated increase in LPS-induced TNF release depended on ATR at 3h but not 6h after LPS exposure.

Discussion

Global gene expression analysis of livers from rats or primary hepatocytes treated with TVX suggested that TVX selectively targets eukaryotic topoisomerases, an off-target effect for a prokaryotic topoisomerase poison (Liguori et al., 2008; Waring et al., 2006). Additionally, TVX affected chromosomal expression patterns in a manner similar to the known eukaryotic topoisomerase poisons, etoposide and doxorubicin, suggesting further that TVX might act as a topoisomerase poison in mammalian cells (Reymann and Borlak; 2008). *In silico* binding analysis (Figure 1) suggested that TVX binds favorably to eukaryotic TopIIa. Moreover, TVX prevented human TopIIa-dependent decatenation of kinetoplastid DNA in a concentration-dependent manner (Figure 2). Taken together, these results raised the possibility that the IDILI liability associated with TVX might be attributed to off-target poisoning of eukaryotic topoisomerase. Topoisomerase inhibition in cells can lead to double-strand DNA breaks (DSBs) generated from topoisomerase-DNA covalent complexes (Drummond et al., 2011; Li et al., 2010; Liu et al., 1983; Ryan et al., 1991). pH2A.X was chosen as a sensitive marker of DSBs. TVX increased pH2A.X in a concentration-dependent manner in RAW cells after a 2-hour incubation (Figure 3A).

TVX is associated with IDILI in humans, whereas LVX does not share this liability (Leitner et al., 2010). In mice, TVX/LPS coexposure precipitated hepatotoxicity, but LVX/LPS did not (Shaw et al., 2007). The results *in silico* (Figure 1) suggested that TVX has the capacity to bind to TopIIa in a distinct manner compared to LVX. Unlike TVX, LVX did not increase pH2A.X (Figure 3B) or increase TNF expression (Poulsen et

al., 2014). Thus, the difference in the association with IDILI for these two drugs was reflected in their abilities to cause modest DNA damage and augment TNF expression as well as to interact with LPS in mice to precipitate liver injury.

A recent screen of novel bacterial type II topoisomerase inhibitors in murine L5178Y lymphoma cells used pH2A.X as an indicator of topoisomerase inhibition (Smart and Lynch, 2012). A substantial proportion (22/63) of the novel inhibitors, as well as CPX and MOX modestly increased pH2A.X in mammalian cells, and this increase coincided with a >6-fold increase in mutation frequency, suggesting that many bacterial topoisomerase inhibitors, including fluoroquinolones like CPX and MOX, can induce weak genotoxic effects in eukaryotic cells (Smart and Lynch, 2012). The phosphorylation of H2A.X that we observed with TVX was quite modest compared to the effect of potent eukaryotic DNA damaging agents (Anderson and Osheroff, 2001; Smart and Lynch, 2012). This modest, otherwise nontoxic damage is consistent with *in vivo* studies with TVX, in the sense that TVX was nontoxic even at large doses in mice in the absence of a concurrent inflammatory stress (Shaw et al., 2007).

Taken together, the results in Figures 1-3 suggest that TVX poisons topoisomerase in RAW cells and that this leads to DNA damage which does not result in cell death. Accordingly, it is likely that the TVX-induced DNA damage is within the capacity of the cells to repair, but the signaling activated in response to DNA lesions predisposes cells to enhance synthesis of TNF in response to LPS. DNA lesions activate several mediators and intracellular signaling pathways in a coordinated and dynamic manner that is referred to as the DNA damage response (DDR) (Ciccia and Elledge, 2010). ATM and ATR are rapidly activated kinases that are critical to the DDR

(Kastan et al., 2000). Treatment with TVX caused an increase in phosphorylation of an epitope in proteins (Figure 4A) that is a target for both ATM and ATR (Kim et al., 1999). This occurred prior to pH2A.X generation (Figure 3), and ATM and ATR inhibitors prevented TVX-induced phosphorylation of this epitope (Figure 4B), suggesting that TVX exposure activated ATM and ATR. The results in Figures 1 - 4 support a scenario in which TVX poisons eukaryotic topoisomerase, damages DNA and activates DDR kinases.

A large amount of evidence supports a link between induction of DNA damage and upregulation of cytokine expression. For example, potent eukaryotic topoisomerase poisons doxorubicin and etoposide, as well as the anti-metabolite 5-fluorouracil, can increase cytokine expression in murine macrophages in vitro and in mice in vivo (Elsea et al., 2008; Wood et al., 2006). The increase in TNF mRNA caused by TVX in RAW cells was sensitive to inhibition of ATR but unaffected by inhibition of ATM and to nonselective PI3K inhibition by WORT (Figure 5A). ATR is far less sensitive to inhibition by WORT than ATM or DNA-PK (Sarkaria et al., 1998), so it was likely that the enhanced TNF expression was downstream of ATR-mediated signaling. Thus, although several PI3Ks, including ATM, ATR and DNA-PK, are activated in response to DNA lesions (Ciccia an Elledge, 2010), only ATR was implicated in the enhancement of TNF expression by TVX. TNF mRNA rapidly degrades in the absence of an inflammatory stimulus (Deleault et al., 2008). Interestingly, treatment with TVX stabilized TNF mRNA prior to LPS exposure (Figure 5B), and NU6027 markedly reduced this effect, suggesting that TVX-dependent ATR activation stabilizes TNF mRNA.

Since ATR was implicated in the TVX-induced increase in TNF mRNA (Figure 5), the involvement of ATR in LPS-induced TNF protein release was examined. KU55933 and NU6027 were included only during the period of exposure to TVX and were removed before addition of LPS or SAL. This was done to determine if the critical TVX-induced signaling changes occurred prior to LPS exposure. TVX pretreatment enhanced LPS-induced TNF protein release within 3h after LPS addition, and this increase was prevented by NU6027 (Figure 6A). When NU6027 was added after LPS addition, the TVX-mediated potentiation of TNF release was not prevented (Supplemental Figure 1). Accordingly, the critical ATR activation must have occurred during the TVX pretreatment period, not after LPS addition. Elimination of the LPS-TVX interaction by NU6027 was evident 3h after LPS addition, but not at 6h (Figure 6B). One potential explanation for the lack of effect at 6 h is that ATR could be activated after withdrawal of NU6027-containing medium if the DNA damage persists during the time of LPS exposure.

The effect of TVX on cytokine expression has been addressed in two other studies (Khan et al., 1998; Purswani et al., 2000). In both of these studies, TVX decreased TNF expression in LPS-pretreated cells (Khan et al., 1998; Purswani et al., 2000), contrasting with the increase identified in this study. A key difference in those studies is that TVX was added to monocytes or peripheral mononuclear cells after stimulation with LPS, whereas in our study TVX was present only before LPS addition. In both of the studies in which TVX decreased TNF mRNA and protein release, the results were attributed to TVX acting as a topoisomerase inhibitor in eukaryotic cells (Khan et al., 1998; Purswani et al., 2000). Accordingly, the difference between the

results could be due to temporal differences in TVX exposure relative to LPS. As the results from the current study indicate, the TVX-mediated DDR and consequent activation of ATR before LPS exposure appears to be critical for the TVX-mediated increase in LPS-induced TNF release.

Taken together, the results of *in silico,* cell-free and cultured cell approaches indicate that TVX, but not LVX, can decrease topoisomerase activity and induce DNA damage at concentrations that approach those occurring in patients treated with TVX (Teng et al., 1996). TVX activated ATM/ATR-dependent signaling, and ATR played a critical role in mediating increased TNF mRNA stability and LPS-induced TNF protein release from macrophages. The results from this study uncovered a previously unknown role for the DDR and specifically ATR in increasing TNF expression by macrophages exposed to a modest genotoxic stimulus. The results suggest that topoisomerase inhibition might contribute to IDILI caused by TVX and perhaps other fluoroquinolone antibiotics.

Authorship Contributions

Participated in research design: Poulsen, Olivero, Beggs, Ganey and Roth

Conducted experiments: Poulsen, Olivero and Beggs

Performed data analysis: Poulsen and Olivero

Wrote or contributed to the writing of the manuscript: Poulsen, Olivero, Ganey and Roth

References

Albertini S, Chetelat AA, Miller B, Muster W, Pujadas E, Strobel R and Gocke E (1995) Genotoxicity of 17 gyrase- and four mammalian topoisomerase II-poisons in prokaryotic and eukaryotic test systems. *Mutagenesis* **10**(4): 343-351.

Anderson VE and Osheroff N (2001) Type II topoisomerases as targets for quinolone antibacterials: turning Dr. Jekyll into Mr. Hyde. *Curr Pharm Des* **7**(5): 337-353.

Barrett JF, Gootz TD, McGuirk PR, Farrell CA and Sokolowski SA (1989) Use of in vitro topoisomerase II assays for studying quinolone antibacterial agents. *Antimicrob Agents Chemother* **33**(10): 1697-1703.

Bates AD, Berger JM and Maxwell A (2011) The ancestral role of ATP hydrolysis in type II topoisomerases: prevention of DNA double-strand breaks. *Nucleic Acids Res* **39**(15): 6327-6339.

Brighty KE and Gootz TD (1997) The chemistry and biological profile of trovafloxacin. *J Antimicrob Chemother* **39** Suppl B: 1-14.

Ciccia A and Elledge SJ (2010) The DNA damage response: making it safe to play with knives. *Mol Cell* **40**(2): 179-204.

Deleault KM, Skinner SJ and Brooks SA (2008) Tristetraprolin regulates TNF TNF-alpha mRNA stability via a proteasome dependent mechanism involving the combined action of the ERK and p38 pathways. *Mol Immunol* **45**(1): 13-24.

Drummond CJ, Finlay GJ, Broome L, Marshall ES, Richardson E and Baguley BC (2011) Action of SN 28049, a new DNA binding topoisomerase II-directed antitumour drug: comparison with doxorubicin and etoposide. *Invest New Drugs,* **29**(5): 1102-1110.

Elsea CR, Roberts DA, Druker BJ and Wood LJ (2008) Inhibition of p38 MAPK suppresses inflammatory cytokine induction by etoposide, 5-fluorouracil, and doxorubicin without affecting tumoricidal activity. *PLoS One*. **3**(6):e2355.

Gootz TD and Brighty KE (1996) Fluoroquinolone antibacterials: SAR mechanism of action, resistance, and clinical aspects. *Med Res Rev* **16**(5): 433-486

Guha R, Dutta D, Jurs PC and Chen T (2006) Local lazy regression: making use of the neighborhood to improve QSAR predictions. *J Chem Inf Model* **46**(4): 1836-1847

Herbold BA, Brendler-Schwaab SY and Ahr HJ (2001) Ciprofloxacin: in vivo genotoxicity studies. *Mutat Res* **498**(1-2): 193-205.

Hickson I, Zhao Y, Richardson CJ, Green SJ, Martin NM, Orr AI, Reaper PM, Jackson SP, Curtin NJ and Smith GC (2004) Identification and Characterization of a Novel and

Specific Inhibitor of the Ataxia-Telangiectasia Mutated Kinase ATM. *Cancer Res.* **64**(24): 9152-9159.

Kastan MB, Lim DS, Kim ST, Xu B and Canman C (2000) Multiple signaling pathways involving ATM. *Cold Spring Harb Symp Quant Biol* **65**: 521-526.

Khan AA, Slifer TR and Remington JS (1998) Effect of trovafloxacin on production of cytokines by human monocytes. *Antimicrob Agents Chemother* **42**(7): 1713-1717.

Kim ST, Lim DS, Canman CE and Kastan MB (1999) Substrate specificities and identification of putative substrates of ATM kinase family members. *J Biol Chem* **274**(53): 37538-37543.

Lasser KE, Allen PD, Woolhandler SJ, Himmelstein DU, Wolfe SM, and Bor DH (2002) Timing of new black box warnings and withdrawals for prescription medications. *JAMA* **287**(17): 2215-20.

Leitner JM, Graninger W and Thalhammer F (2010) Hepatotoxicity of antibacterials: Pathomechanisms and clinical. *Infection* **38**(1): 3-11.

Li Y, Luan Y, Qi X, Li M, Gong L, Xue X, Wu X, Wu Y, Chen M, Xing G, Yao J, and Ren J. (2010) Emodin triggers DNA double-strand breaks by stabilizing topoisomerase II-DNA cleavage complexes and by inhibiting ATP hydrolysis of topoisomerase II. *Toxicol*

Sci **118**(2): 435-443.

Liguori MJ, Blomme EA and Waring JF (2008) Trovafloxacin-induced gene expression changes in liver-derived in vitro systems: comparison of primary human hepatocytes to HepG2 cells. *Drug Metab Dispos* **36**(2): 223-233.

Liu LF, Rowe TC, Yang L, Tewey KM and Chen GL (1983) Cleavage of DNA by mammalian DNA topoisomerase II. *J Biol Chem* **258**(24): 15365-15370.

Lu J, Jones AD, Harkema JR, Roth RA and Ganey PE (2012) Amiodarone exposure during modest inflammation induces idiosyncrasy-like liver injury in rats: role of tumor necrosis factor-alpha. *Toxicol Sci* **125**: 126-133.

Ostapowicz G, Fontana RJ, Schiodt FV, Larson A, Davern TJ, Han SH, McCashland TM, Shakil AO, Hay JE, Hynan L, Crippin JS, Blei AT, Samuel G, Reisch J and Lee WM (2002) Results of a prospective study of acute liver failure at 17 tertiary care centers in the United States. *Ann Intern Med* **137**(12): 947-954

Peasland A, Wang LZ, Rowling E, Kyle S, Chen T, Hopkins A, Cliby WA, Sarkaria J, Beale G, Edmondson RJ and Curtin NJ (2011) Identification and evaluation of a potent novel ATR inhibitor, NU6027, in breast and ovarian cancer cell lines. *Br J Cancer* **105**(3): 372-381.

Poulsen KL, Ganey PE and Roth RA (2014) Trovafloxacin Potentiation of Lipopolysaccharide-Induced Tumor Necrosis Factor Release from RAW 264.7 Cells Requires Extracellular Signal-Regulated Kinase and c-Jun N-Terminal Kinase.. *J Pharmacol Exp Ther* **349**(2): 185-191.

Powis G, Bonjouklian R, Berggren MM, Gallegos A, Abraham R, Ashendel C, Zalkow L, Matter WF, Dodge J, Grindey G and Vlahos CJ. (1994) Wortmannin, a potent and selective inhibitor of phosphatidylinositol-3-kinase. *Cancer Res.* **54**(9): 2419-2423.

Purswani M, Eckert S, Arora H, Johann-Liang R and Noel GJ (2000) The effect of three broad-spectrum antimicrobials on mononuclear cell responses to encapsulated bacteria: evidence for down-regulation of cytokine mRNA transcription by trovafloxacin. *J Antimicrob Chemother* **46**(6): 921-929.

Reuveni D, Halperin D, Shalit I, Priel E and Fabian I (2008) Quinolones as enhancers of camptothecin-induced cytotoxic and anti-topoisomerase I effects. *Biochem Pharmacol* **75**(6): 1272-1281.

Reymann S and Borlak J (2008) Topoisomerase II inhibition involves characteristic chromosomal expression patterns. *BMC Genomics* **9:** 324.

Roth RA and Ganey PE (2011) Animal models of idiosyncratic drug-induced liver injury--current status. *Crit Rev Toxicol* **41**(9): 723-739.

Ryan AJ, Squires S, Strutt HL and Johnson RT (1991) Camptothecin cytotoxicity in mammalian cells is associated with the induction of persistent double strand breaks in replicating DNA. *Nucleic Acids Res* **19**(12): 3295-3300.

Sanner MF, Duncan BS, Carrillo CJ and Olson AJ (1999) Integrating computation and visualization for biomolecular analysis: an example using python and AVS. *Pac Symp Biocomput* 401-12.

Sarkaria JN, Tibbetts RS, Busby EC, Kennedy AP, Hill DE and Abraham RT (1998) Inhibition of phosphoinositide 3-kinase related kinases by the radiosensitizing agent wortmannin. *Cancer Res* **58**(19): 4375-4382.

Shaw PJ, Hopfensperger MJ, Ganey PE and Roth RA (2007) Lipopolysaccharide and trovafloxacin coexposure in mice causes idiosyncrasy-like liver injury dependent on tumor necrosis factor-alpha. *Toxicol Sci* **100**(1): 259-266.

Shaw PJ, Beggs KM, Sparkenbaugh EM, Dugan CM, Ganey PE and Roth RA (2009a) Trovafloxacin enhances TNF-induced inflammatory stress and cell death signaling and reduces TNF clearance in a murine model of idiosyncratic hepatotoxicity. *Toxicol Sci* **111**(2): 288-301.

Shaw PJ, Ganey PE, Roth RA (2009b) Tumor necrosis factor alpha is a proximal mediator of synergistic hepatotoxicity from trovafloxacin/lipopolysaccharide coexposure. *J Pharmacol Exp Ther* **328**(1): 62-68.

Shaw PJ, Ganey PE and Roth RA (2010) Idiosyncratic drug-induced liver injury and the role of inflammatory stress with an emphasis on an animal model of trovafloxacin hepatotoxicity. *Toxicol Sci* **118**(1): 7-18

Smart DJ and Lynch AM (2012) Evaluating the genotoxicity of topoisomerase-targeted antibiotics. *Mutagenesis* **27**(3): 359-365

Teng R, Liston TE Harris SC (1996) Multiple-dose pharmacokinetics and safety of trovafloxacin in healthy volunteers. *J Antimicrob Chemother* **37**(5): 955-963.

Trott O, Olson AJ (2010) AutoDock Vina: improving the speed and accuracy of docking with a new scoring function, efficient optimization, and multithreading. *J Comput Chem* **31**(2): 455-61.

Vreven T, Morokuma K, Farkas O, Schlegel HB and Frisch MJ (2003) Geometry optimization with QM/MM, ONIOM, and other combined methods. I. Microiterations and constraints. *J Comput Chem* **24**: 760-769.

Waring JF, Liguori MJ, Luyendyk JP, Maddox JF, Ganey PE, Stachlewitz RF, North C, Blomme EA, Roth RA (2006) Microarray analysis of lipopolysaccharide potentiation of trovafloxacin-induced liver injury in rats suggests a role for proinflammatory chemokines and neutrophils. *J Pharmacol Exp Ther* **316**(3): 1080-1087.

Wood LJ, Nail LM, Perrin NA, Elsea CR, Fischer A and Druker BJ (2006) The cancer chemotherapy drug etoposide (VP-16) induces proinflammatory cytokine production and sickness behavior-like symptoms in a mouse model of cancer chemotherapy-related symptoms. *Biol Res Nurs* **8**(2): 157-169.

Zou W, Beggs KM, Sparkenbaugh EM, Jones AD, Younis HS, Roth RA and Ganey PE (2009) Sulindac metabolism and synergy with tumor necrosis factor-alpha in a drug-inflammation interaction model of idiosyncratic liver injury. *J Pharmacol Exp Ther* **331**(1): 114-121.

Footnotes

This study was supported by National Institutes of Health [DK061315]. KLP was supported by National Institute of Environmental Health Sciences Training Grant [T32ES007255].

Figure Legends

Figure 1. *In silico* analysis of TVX binding to TopIIa. A) Theoretical binding sites for TVX on TopIIa molecule are shown with binding affinities displayed in Kcal/mol. **B)** Theoretical frequency of occupation (BF; the number of docking runs in which the drug bound to a site) for TVX in sites 1 and 2. **C)** Theoretical binding sites for LVX on TopIIa molecule are shown with binding affinities displayed in Kcal/mol. **D)** Theoretical frequency of occupation for LVX in sites 1-3. For explanation of analysis and calculations, see Methods.

Figure 2. Effect of TVX on TopIIa activity. A reaction mixture containing kinetoplastid DNA (kDNA) in the absence (1st lane on the left; kDNA) or presence of TopIIa (all other lanes) was incubated with 0 (VEH), 10, 30, 100 or 300 µM TVX or 10 µM VP-16. After 30 minutes, the reaction was quenched, and samples were separated on a 1% agarose gel and stained with ethidium bromide to visualize DNA decatenate migration. **Image is representative from a minimum of n=3.**

Figure 3. TVX-induced DNA damage in RAW cells. A) RAW cells were exposed to vehicle (VEH) or TVX (1-300 µM) for 2 hours. pH2A.X was assessed in protein extracts by western blot. Signals for pH2A.X were densitized and normalized to actin. **B)** RAW cells were exposed to TVX (100 µM) or LVX (300 µM) for 2 hours. pH2A.X induction was assessed in protein extracts. Signals for pH2A.X were densitized and normalized to actin. Blots are representative from a minimum of n=3. a - Significantly different from VEH, $p<0.05$.

JPET Fast Forward. Published on May 9, 2014 as DOI: 10.1124/jpet.114.214189
This article has not been copyedited and formatted. The final version may differ from this version.

Figure 4. ATM and ATR activation by TVX in RAW cells. A) RAW cells were exposed to VEH or TVX (100 µM) for 1 or 2 hours. pATM/ATR substrate motif was assessed in isolated protein extracts by western analysis, and signal was densitized and normalized to lamin B1. **B)** RAW cells were exposed to VEH or TVX (100 µM) and to ATM inhibitor KU55933 (1 µM), ATR inhibitor NU6027 (10 µM) or their DMSO (0.05%) vehicle for 1 hour. pATM/ATR substrate motif was assessed in isolated protein extracts by western analysis and normalized to lamin b1. Blots are representative from a minimum of n=3. a - Significantly different from VEH, $p<0.05$.

Figure 5. ATR-dependent expression of TNF mRNA in response to TVX. A) RAW cells were coexposed to VEH or TVX (100 µM) and to WORT (1 µM), KU55933 (1 µM), NU6027 (10 µM) or their DMSO (0.05%) vehicle for 2 hours. TNF mRNA was assessed by RT-PCR. Values are expressed as fold of VEH/DMSO ± SEM or VEH/Inhibitor ± SEM, n=3-6. a - $p<0.05$ vs. VEH group with same inhibitor, b - $p<0.05$ vs. TVX/DMSO. **B)** RAW cells were exposed to TVX (100 µM) or its VEH and to NU6027 (10 µM) or its DMSO (0.05%) vehicle for 1 hour before addition of ActD (5 µg/ml), and RNA was isolated at indicated times after ActD. TNF mRNA was normalized to the t = 0 value for each group. Values are expressed as %TNF remaining ± SEM, n=6. a - $p<0.05$ vs. VEH/DMSO at the same time, b - $p<0.05$ vs. TVX/DMSO at the same time

JPET Fast Forward. Published on May 9, 2014 as DOI: 10.1124/jpet.114.214189
This article has not been copyedited and formatted. The final version may differ from this version.

Figure 6. Effect of ATM and ATR inhibition on TVX-mediated increases in LPS-induced TNF release from RAW cells. RAW cells were pretreated with VEH or TVX (100 μM) and with NU6027 (10 μM), WORT (1 μM), KU55933 (1 μM), or their DMSO (0.05%) vehicle for 2 hours, after which time medium was replaced with one containing SAL or LPS (10 ng/ml) without inhibitors. TNF protein release was assessed at **A)** 3h **B)** 6h after LPS exposure. Values are means ± SEM from 3-6 separate experiments, each performed in triplicate. a - Significantly different from VEH/SAL with same inhibitor treatment, $p<0.05$, b – Significantly different from VEH/LPS with same inhibitor treatment, $p<0.05$, c – Significantly different from TVX/SAL/DMSO group, $p<0.05$, d – Significantly different from TVX/LPS/DMSO group, $p<0.05$.

JPET Fast Forward. Published on May 9, 2014 as DOI: 10.1124/jpet.114.214189
This article has not been copyedited and formatted. The final version may differ from this version.

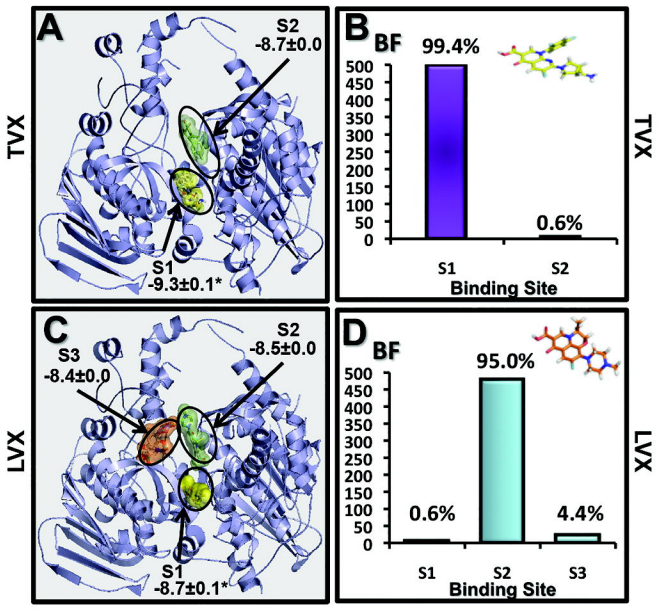

FIGURE 1

JPET Fast Forward. Published on May 9, 2014 as DOI: 10.1124/jpet.114.214189
This article has not been copyedited and formatted. The final version may differ from this version.

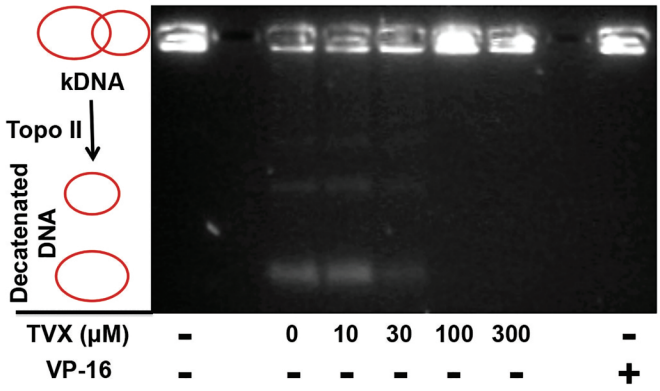

FIGURE 2

JPET Fast Forward. Published on May 9, 2014 as DOI: 10.1124/jpet.114.214189
This article has not been copyedited and formatted. The final version may differ from this version.

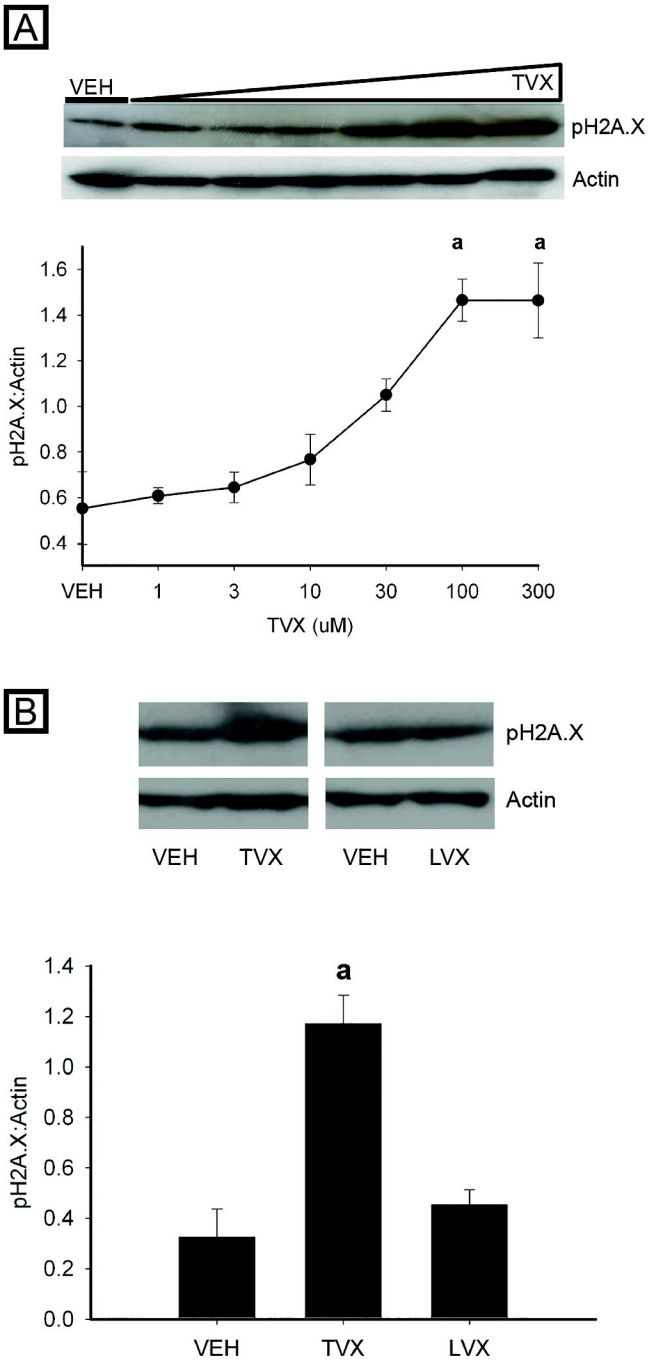

FIGURE 3

JPET Fast Forward. Published on May 9, 2014 as DOI: 10.1124/jpet.114.214189
This article has not been copyedited and formatted. The final version may differ from this version.

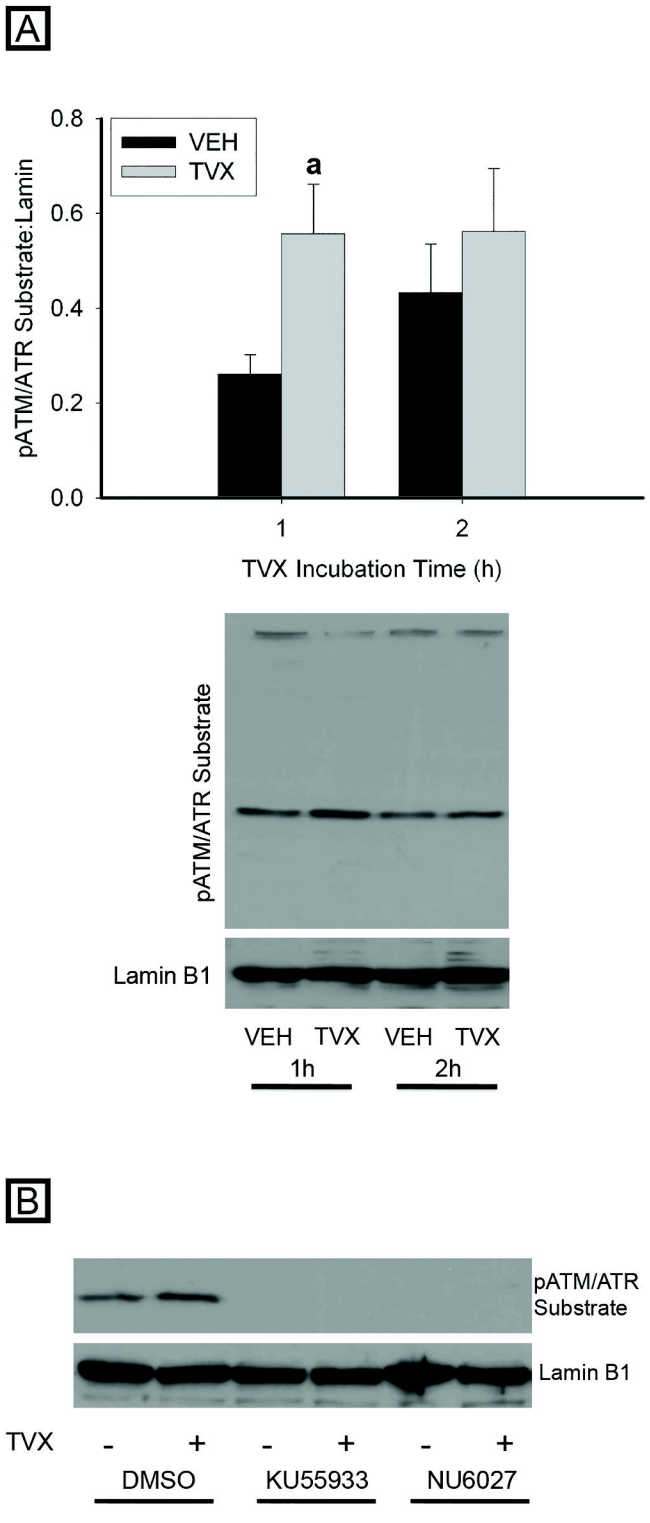

FIGURE 4

JPET Fast Forward. Published on May 9, 2014 as DOI: 10.1124/jpet.114.214189
This article has not been copyedited and formatted. The final version may differ from this version.

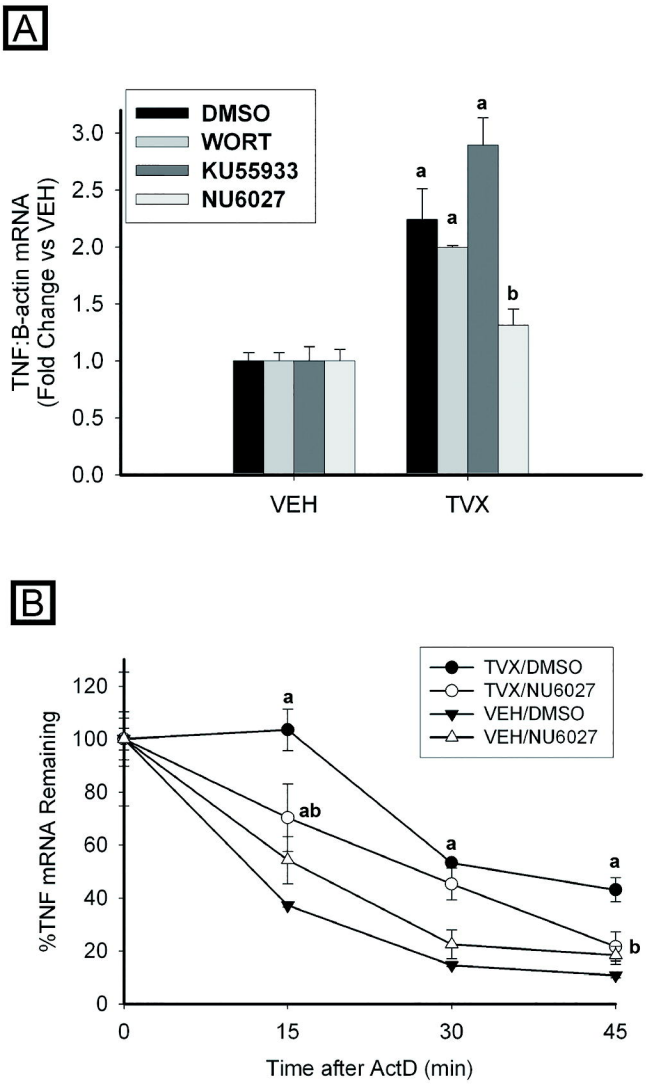

FIGURE 5

JPET Fast Forward. Published on May 9, 2014 as DOI: 10.1124/jpet.114.214189
This article has not been copyedited and formatted. The final version may differ from this version.

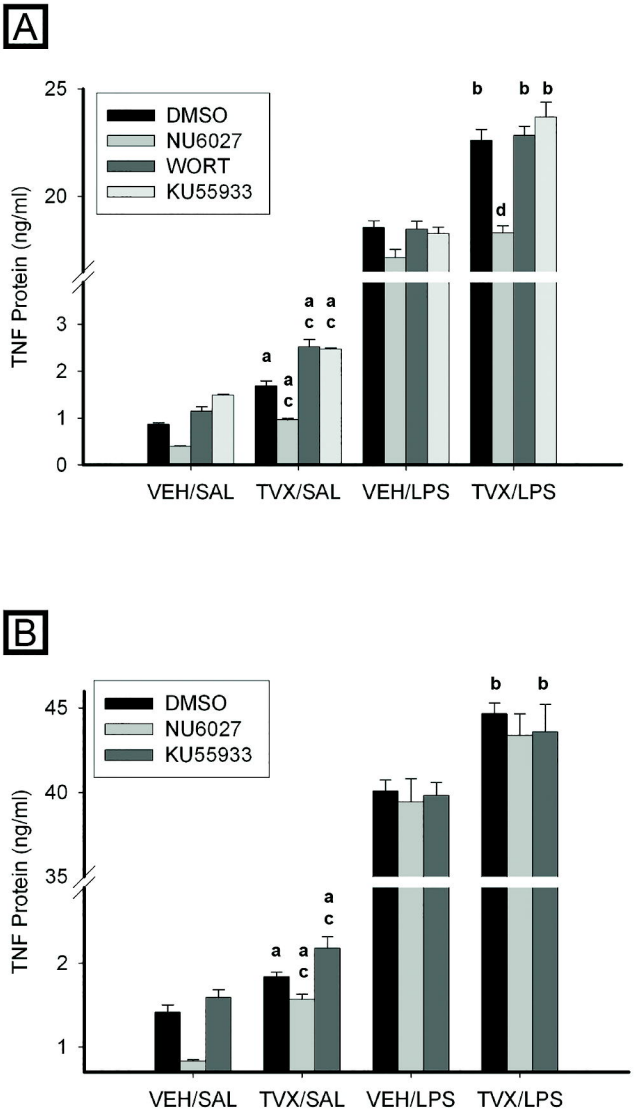

FIGURE 6